UNUSUAL TECHNIQUES AND NEW APPLICATIONS OF METALLOGRAPHY

Edited by
R. J. Gray and L. R. Cornwell

Serving the World
of Materials Technology

Conference Proceedings
Metallography Series
Volume I

UNUSUAL TECHNIQUES AND NEW APPLICATIONS OF METALLOGRAPHY

Volume 1

Edited by

R. J. Gray and L. R. Cornwell
Department of Mechanical Engineering
Texas A&M University
College Station, Texas

Papers taken from the Metallography Symposia
held at the ASM Metals Congress
St. Louis, Missouri, 27 October 1982
and
Philadelphia, Pennsylvania, 4–5 October 1983

Sponsored by

American Society for Metals
International Metallographic Society

Published by

Cover art shows Ultrathin sections of Mount St. Helens ash using reflected light and transmitted polarized light (Fig. 8 — Paper 8305-021—R. H. Beauchamp & J. F. Williford)

Library of Congress Catalog Card Number: 85-071946

ISBN: 0-87170-209-6

SAN: 204-7586

Printed in the United States of America

Printed and Bound by Publishers Choice Book Mfg. Co.
Mars, Pennsylvania 16046

PREFACE

The Metallographic Committee of the Materials Testing and Quality Control Technical Division of ASM felt there was a need to include a session on Metallography at ASM Metals Congress which is normally held in the Fall. Since a large number of managers, engineers and shop floor personnel attend this Congress, it seemed a good way to provide the opportunity for exposure to new techniques in Metallography. Also covered in the sessions was the application of conventional metallographic methods in new areas.

The first Symposium was held in St. Louis on October 27 and 28, 1982 with the emphasis on the application of metallography to identifying microstructures in welding and superalloys. The second Symposium was held in Philadelphia on October 4 and 5, 1983 and the topics covered there included the application of metallography to electronic components and to steelmaking process control. At both Symposia, papers were presented based on entries to the International Metallographic Exhibit. It is felt that this will provide more exposure for some of the entries which can tell an interesting story or illustrate ingenious ways of using metallography to solve a problem.

The Symposia were sponsored by the American Society for Metals and the International Metallographic Society. A Symposium was held at the Metals Congress in Detroit in September 1984 and another one will be held at the next Metals Congress in Toronto in 1985. It is hoped that this first volume will have sufficient appeal to justify publishing the Symposium proceedings in this manner each year.

R. J.Gray
L. R. Cornwell

(The following papers were presented at the 1982/'83 ASM Metals Congresses but were unavailable in manuscript form for publication)

1982 Metals Congress:

An Overview of the Metallography of Joining Materials
C. Lundin, University of Tennessee, Knoxville, Tennessee, U.S.A.

Metallographic Examinations of Welds in the Field
R. J. Gray, B. C. Leslie, Oak Ridge National Laboratory, Oak Ridge, Tennessee, U.S.A.

Ghosts from the Past in JBK-75 Stainless Steel
M. J. Carr, M. C. Mataya, N. Wilkenson, W. L. Johns, J. M. Steele, Rockwell International, Golden, Colorado, U.S.A.

Characteristics of 440 A Grinding Swarf
H. Chang, B. Alexander, Gillette Company, Boston, Massachusetts, U.S.A.

Changes in Impact Toughness of Type 316 Stainless Steel Due to Thermal Aging or Service -- Is Predictable Based on Equivalent Microstructures
V. R. Sikka, J. M. Vitek, S. A. David, Oak Ridge National Laboratory, Oak Ridge, Tennessee, U.S.A.; F. Ellis, Combustion Engineering, Inc., Chattanooga, Tennessee, U.S.A.

Metallographic Study of Strengthening Mechanisms in a Hardenable 16Cr-1.5Mo-5Ni Stainless Steel
V. Biss, P. J. Grobner, Climax Molybdenum Company of Michigan, Ann Arbor, Michigan, U.S.A.

Developments in the Use of Marshall's Reagent for Low Carbon Steels
A. O. Benscoter, (G. Vander Voort) Bethlehem Steel Corporation, Bethlehem, Pennsylvania, U.S.A.

JK Inclusion Ratings by Image Analysis
J. F. Golden, E. Leitz Inc., G. Vander Voort, Bethlehem, Pennsylvania, U.S.A.

Understanding of Superalloys Through Metallography
W. J. Boesch, F. J. Warmuth, Special Metals, New Hartford, New York, U.S.A.

Metallography of Superalloys: Preparation and Interpretation
T. Sanders, J. F. Radavich, Purdue University, Lafayette, Indiana, U.S.A.

Superalloy Microstructures: Preparation for Scanning ELectron Metallography
G. J. Stelma, S. O. Mancuso, J. A. Domiongue, Special Metals, New Hartford, New York, U.S.A.

Metallographic Techniques and Structure Interpretation in Cobalt-Base Superalloys
M. F. Rothman, R. B. Herchenroeder, J. A. Martin, R. D. Zordan, Cabot Corporation, Kokomo, Indiana, U.S.A.

TEM/STEM Microscopy of Superalloys
R. N. Jarrett, R. D. Kissinger, J. K. Tien, Columbia University, N. Y., U.S.A.

1983 Metals Congress:

Application of Unusual Metallographic Techniques to the Study of Grain Boundary Cavitation in Nickel + 1% Sb
C. L. White, R. A. Padgett, Jr., Oak Ridge National Laboratory, Oak Ridge, Tennessee, U.S.A.

Colored Metallographic Techniques at Lawrence Livermore Laboratories
D. J. Diaz, Lawrence Livermore National Labs., Livermore, California, U.S.A.

Substructure Effects on the Mechanical Behavior of 16-8-2 Weld Metal
J. R. Foulds, GA Technologies, Inc., San Diego, California, U.S.A.;
J. Moteff, University of Cincinnati, Cincinnati, Ohio, U.S.A.

Relationship Between Microstructure and Impact Energy of Aged CF8M Steel
B. R. Patterson, University of Alabama in Birmingham, Birmingham, Alabama, U.S.A.; W. D. Morrow, Alabama Power Company, Birmingham, Alabama, U.S.A.

Micromechanical and Microstructural Evaluation of Stainless Steel Overlays on Low Alloy Steel Plate
J. Moteff, E. Rosa, P. Choi, University of Cincinnati, Cincinnati, Ohio, U.S.A.

Mechanical Properties and Microstructure of an Electroslag Cast Stainless Steel Body
V. K. Sikka, Oak Ridge National Laboratory, Oak Ridge, Tennessee, U.S.A.;
Y. L. Hotsur, Union Carbide Corporation, Oak Ridge, Tennessee, U.S.A.

Refining of Steel Melts by Filtration
S. Ali, D. Apelian, R. Mutharasan, Drexel University, Philadelphia, Pennsylvania, U.S.A.

Inclusion in Ca-Treated Steels
G. Vander Voort, Bethlehem Steel Corporation,. Bethlehem, Pennsylvania, U.S.A.

Application of the Metallographic Cross Section of Microelectronics and Semiconductors
J. R. Devaney, Hi-Rel Laboratories, Monrovia, California, U.S.A.

Analysis of Printed Circuit Boards Cross-Sectional
J. A. Nelson, Buehler Ltd., Lake Bluff, Illinois, U.S.A.

TABLE OF CONTENTS

The numbers indicated in parenthesis following each paper in the Table of Contents and appearing on the first page of each paper are for the ASM Metals/Materials Technology Series paper system and should be referenced to order individual papers.

INTERFERENCE LAYER METALLOGRAPHY OF JOINING MATERIALS

Dr. I. Aydin
Deloro Stellite GmbH
P.O.B. 520
D - 5400 Koblenz

Prof. Dr. H.-E. Buehler
Didier-Werke AG
Lessingstrasse 16-18
D - 6200 Wiesbaden

ABSTRACT

In metal-metal or metal-ceramic composites, combinations of materials are often used in which the different components have widely differing optical properties. Highly reflecting metals and practically absorption-free oxides must therefore be differentiated by means of an adequate light-dark or colour contrast. As examples of joining material systems have been selected:

a) surface treated steels (steel-aluminium),
b) plasma layers,
c) braze joints,
d) metal-ceramic composites

These examples demonstrate in characteristic fashion the possibilities of alloying and processing techniques, but they also give an insight into the application of interference metallography in all those cases in which the phases to be examined have widely differing optical properties. The determination of optical constants for several groups of materials aids to identify all phases by refractive index and absorption coefficient. Today, a lot of constants are well known and it is important to note, that we did not find two phases which have exactly the same optical properties. That means that interference layer metallography is able to separate all phases in one specimen in a reproducible good light-dark contrast and, in most cases also in a good colour contrast.

INTRODUCTION

The aim if a metallographic preparation is to fix the light-dark contrast and the colour contrast between the various phases reproducibly. In this range of metallography remarkable progress was made in the recent two decades with the help of the interference layer procedure. At this point a detailed description of the effects and methods can be ommitted. It is refe-red to the extensive literature available (1-10).

By applying interference layers on a polished surface the fact is reached that according to equation (1) both the light-dark contrast between the various phases can be increased, and the colour contrast enables a quantitative description of colour differences between structural constituents when applying equation (2).

$$R_M = \left[\frac{q_1 \cdot q_2}{1 - q_1 \cdot q_2}\right]^2 \qquad (1)$$

$$tg\delta = \frac{2n_s \cdot k_p}{n_s^2 - n_p^2 - k_p^2} \qquad (2)$$

Necessary condition for the application of equations (1) and (2) is the knowledge of the optical constants n_p and k_p of the phases . In equation (1):

$$q_1 = \frac{n_s - 1}{n_s + 1} \qquad (1a)$$

$$q_2^2 = \frac{(n_p - n_s)^2 + k_p^2}{(n_p + n_s)^2 + k_p^2} \qquad (1b)$$

Are these constants known, the material with refractive index n_A can be selected from equation (3),

$$n_A^2 = n_p + \frac{k_p^2}{n_p - 1} \qquad (3)$$

which enables the reflectivity R_M of a phase to be reduced to zero. Equation (3) applies to those layer materials which are practically absorption free in the visible wavelength range. If the sputtered or vapor deposited layers have a significant self absorption (which is very often the case) the calculation of R_M becomes more difficult. However, ways to solve this problem are known and reference is made to the corresponding literature (6 and 11).

The interference layer procedure is the only metallographic preparation method guaranteeing a geometrical reproducibility. This means, that polished material surfaces cannot be attacked by etching and that in this way all phases will be reproduced in their true form, size and distribution.

No other preparation method can reach this advantage so invaluable for metallography.

LIGHT-DARK CONTRAST

A mathematical analysis shows that the minimum of reflectivity in coated condition R_M and the optical constants n_p and k_p of the phases to be examined are related by circular equations. This applies to non-absorbing layer materials; with absorbing materials functions almost similar to circles are to be expected.

In fig. 1 such circular functions are shown in which various layers (vapor deposited or sputtered) reduce the reflectivity of phases after coating to zero for any refractive index or absorption coefficient combination. This corresponds to the fulfillment of the amplitude condition, i.e. the amplitude of the incoming waves equals the amplitude of the outgoing wave, so that maximum extinction occurs.

It has to be the aim of quantitative metallography to determine the optical constants k_p and n_p of the various phases. By plotting the calculated values into fig. 1 this will lead automatically to the layer material which will reduce the corresponding phase in its reflectivity to a minimum. Thus a high light-dark contrast would be given which could be fixed reproducibly.

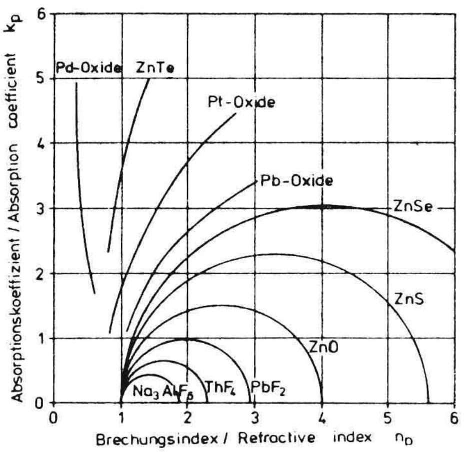

Schicht Layer	n_s	k_s
Pd-Oxide	2,75	0,6
Pt-Oxide	2,75	0,25
Pb-Oxide	2,67	0,1
ZnTe	3,25	0,4
ZnSe	2,65	-
ZnS	2,36	-
ZnO	2,0	-
PbF_2	1,7	-
ThF_4	1,5	-
Na_3AlF_6	1,35	-

$\lambda = 500 - 550$ nm

Fig. 1. Fulfillment of the amplitude condition ($R_M=0$) by non-absorbing layer materials[8]).

In the same way the phase angle δ can be found by plotting n_p and k_p into a n-k-diagramme. This angle allows, e.g. with ZnS vapor deposition as shown in fig. 2, to correctly define the values for the chroma of a phase and/or the chroma differences between various phases.

Colour Contrast

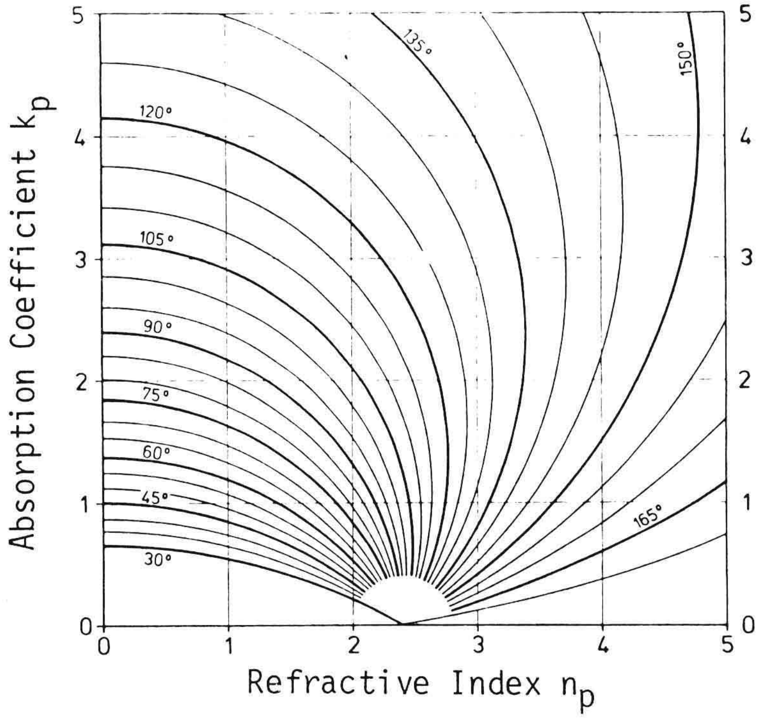

Fig. 2. Determination of phase angles of various phases, realization of the optical constants n_p and k_p (coating with ZnS, λ = 550 nm)

RESULTS WITH JOINING MATERIALS

The following examples of joining materials were examined:

a) Surface-treated steel (hot aluminized with aluminium and/or aluminium-silicium),

b) Plasma sprayed layers,

c) Brazed joints,

d) Metal-ceramic composites

A) Surface-treated steels (compound systems steel-aluminium and steel-(aluminium-silicium))

The phases obtained by hot aluminizing in the diffusion area of steel-aluminium and/or steel-aluminium-silicium are sufficiently known from the literature (12). Thus, with hot aluminized sheets without addition of silicium to aluminium the following phase-sequence can be observed: steel - intermetallic compound Fe_2Al_5 - aluminium. When adding 8 to 10% silicium to aluminium the following phases can be observed on polished surface: steel - α-AlFeSi-(aluminium solid solution, silicium, α-AlFeSi).

The optical constants of these phases are widely known and are shown in fig. 3.

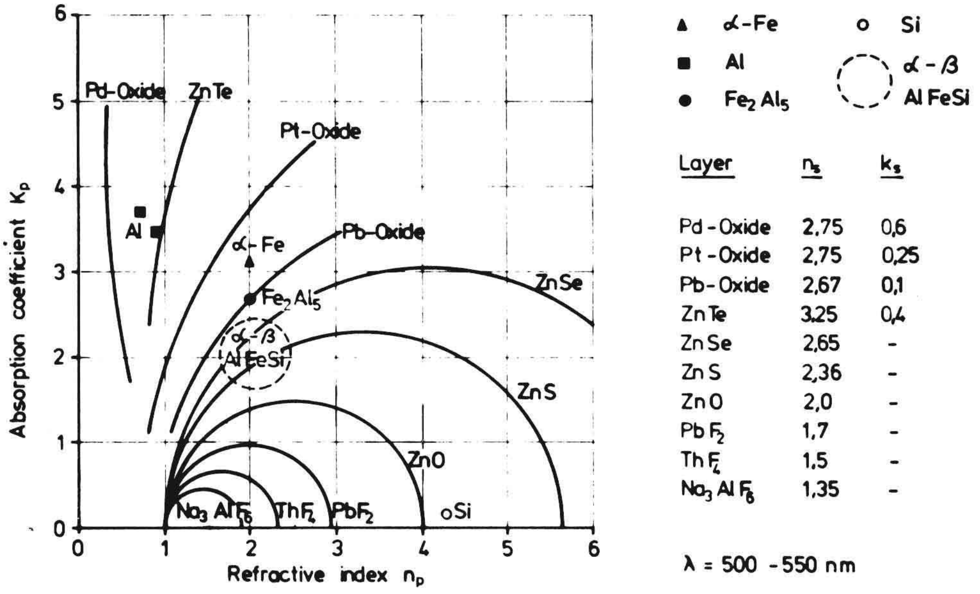

Layer	n_s	k_s
Pd-Oxide	2,75	0,6
Pt-Oxide	2,75	0,25
Pb-Oxide	2,67	0,1
ZnTe	3,25	0,4
ZnSe	2,65	-
ZnS	2,36	-
ZnO	2,0	-
PbF_2	1,7	-
ThF_4	1,5	-
Na_3AlF_6	1,35	-

λ = 500 - 550 nm

Fig. 3. Filfilling the amplitude condition by non-absorbing and absorbing layer materials

When vapor depositing ZnSe on a polished surface of hot aluminized thin sheet (aluminium coating), a microstructure will form under the light-microscope as shown in fig. 4. The aluminium appears rather light, the intermetallic compound Fe_2Al_5 dark grey and α-Fe (steel) light grey. In retrospection to fig. 3 this result becomes clear. When vapor depositing ZnSe, Fe_2Al_5 is next to the circle-line for $R_M=0$, followed by α-Fe. Aluminium has optical constants which are so far away from the other phases (very high self-absorption), that no significant reduction of reflection is to be expected.

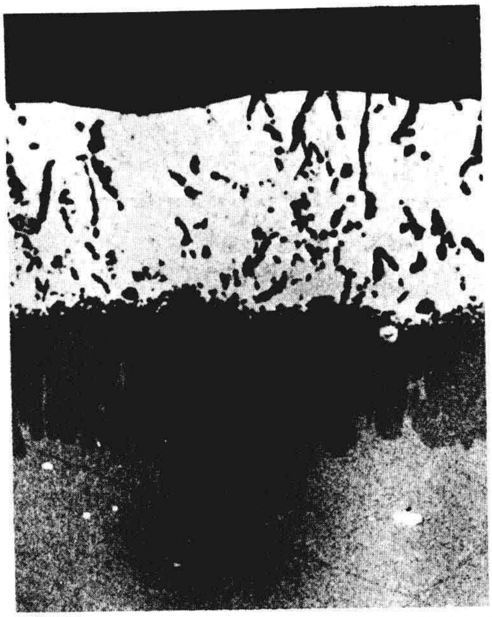
500 : 1

Fig. 4. Hot aluminized sheet (no addition of silicon to aluminium bath)

Polished, vacuum deposited ZnSe layer, zero order, reflection minimum of steel lies at 540 nm, photographed at 540 nm,
steel : dark grey
Fe_2Al_5 : black
aluminium surface layer: white
(embedded Fe_2Al_5 crystallites: black)

The contrast relations can equally well be explained when adding silicium to the aluminium-bath. A coloured picture taken after vapor depositing ZnSe shows the individual phases in the following colours (interference minima of the α-Fe at $\lambda = 580$ nm):

α-AlFeSi: blue-violet in the aluminium-matrix and in the
diffusion area.

steel (α-Fe): blue

silicium: brown

aluminium: light grey-brown

Since this polished surface was vapor deposited with ZnSe in the same way as shown in fig. 4, it would be expected (according to the data given in fig. 3) that α-AlFeSi will be almost extinguished by this kind of coating. Besides, it is to be expected that α-Fe will also undergo a considerable reduction of reflection but that aluminium and silicium will experience merely little reduction of reflection. These expectations are confirmed by the microphotos of fig. 5.

1000 : 1

Fig. 5. Hot aluminized sheet with an aluminium-silicon surface layer

Polished, vacuum deposited ZnSe layer, photographed at 540 nm.
steel and α-AlFeSi : black
aluminium-silicon solid solution : white
silicon : medium grey

So in this case one has almost extinguished the phases -AlFeSi and -Fe after coating with ZnSe. Should, however, aluminium and/or silicium be extinguished, one would have to provide a coating with Pd-oxide or ZnTe for aluminium. As for the silicium it seems to be appropriate to have a ZnO coating.

These explanations are only valid for the case where the reflectivity and the optical constants of the phases do not change considerably in the wavelength between 450 and 600 nm. Besides, the interference minima of the individual phases should spectrally not be too far from each other. This is not the case for all mentioned phases (e.g. silicium), however, fig. 3 supplies useful information to estimate the contrasts between the various phases.

B) Plasma sprayed layers

As regards the plasma sprayed layer, an example is chosen where an unalloyed steel was coated with a sprayed layer, consisting of 50% Fe and 50% Fe_3O_4. The microstructure of the polished and the coated specimen is shown in fig. 6. One can realize that Fe_3O_4 reflects definitely less and therefore the polished surface can clearly be distinguished from the highly reflective iron. After coating significant light-dark contrasts and colour contrasts appear (13).

Fig. 6a 500 : 1

Fig. 6b 500 : 1

Fig. 6. Steel St 37 with a plasma sprayed layer of 50% Fe and 50% Fe_3O_4

To fig. 6a:

Specimen polished,
bright field
steel matrix : white
iron in the plasma layer:
white
Fe_3O_4 : grey
pores : black

To fig. 6b:

Same specimen and area of the microstructure as in fig. 6a, vacuum deposited PbF_2 layer, reflection minimum of steel at 520 nm, bright field
steel matrix: grey
iron in the plasma layer:
: grey
Fe_3O_4 : dark grey, black
pores : black

If you wonder which layer material to choose in this case in order to obtain a best possible light-dark contrast, it is referred to the results of fig. 7. The optical constatns of Fe and Fe_3O_4 reveal that Fe_3O_4 is best extinguished by a vapor deposition of PbF_2 as was the case in fig. 6b. On the reverse, a sputtering with Pb-oxide would lead to an almost complete extinction of the reflectivity of Fe. In this case, by over-fulfillment of the amplitude condition, the Fe_3O_4 would appear light.

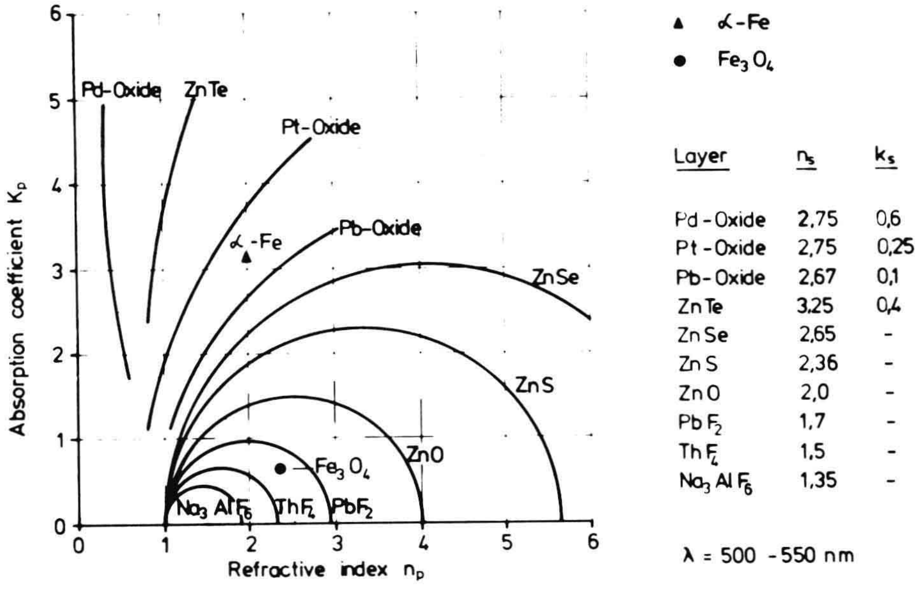

Layer	n_s	k_s
Pd-Oxide	2,75	0,6
Pt-Oxide	2,75	0,25
Pb-Oxide	2,67	0,1
ZnTe	3,25	0,4
ZnSe	2,65	-
ZnS	2,36	-
ZnO	2,0	-
PbF_2	1,7	-
ThF_4	1,5	-
Na_3AlF_6	1,35	-

λ = 500 - 550 nm

Fig. 7. Fulfilling the amplitude condition by non-absorbing and absorbing layer materials

This contrast inversion to be expected to be expected is realized in fig. 8. In this case a nickel layer was sprayed on steel St 37. On applying the spray layer, oxide phases are formed apart from the nickel coating.

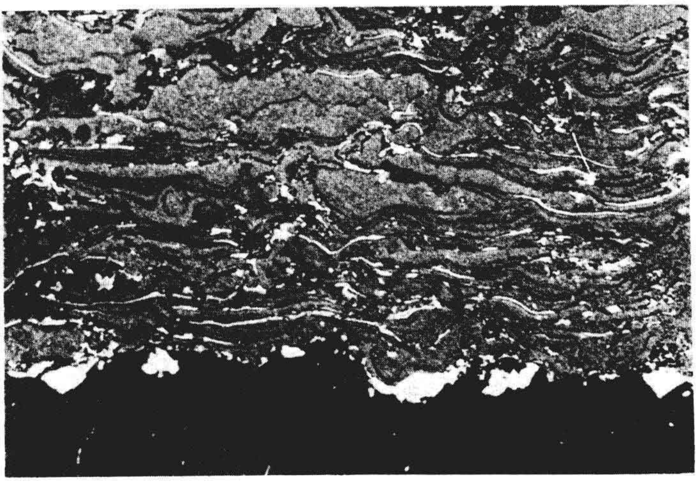

200 : 1

Fig. 8. Plasma sprayed layer on St 37

Specimen sputtered with an iron cathode using oxygen as reaction gas, zero order, reflection minimum of steel at 485 nm, bright field
steel matrix : dark grey
nickel layer : light to medium grey
oxides : white and dark grey

The polished specimen was coated with Fe-oxide (optical characteristics to be found between Pt-oxide and Pd-oxide). According to the statement of fig. 7 the oxide phases now appear light, whereas the metallic phases appear dark. Due to the higher reflective and more absorbing oxide sputter layer, the amplitude condition for the metallic phases is better fulfilled than for the oxide ones. Consequently the expected reversed contrast results. Besides, it is to be seen that the α-Fe (steel St 37) is being more extinguished than the applied nickel coating. This result is, due to the optical constants of iron, nickel and the applied layer material also to be expected (fig. 9).